Int. J. Electrochem. Sci., 10 **(20145)** 272 - 286

International Journal of
ELECTROCHEMICAL
SCIENCE
www.electrochemsci.org

Fast Immobilization of Glucose Oxidase on Graphene Oxide for Highly Sensitive Glucose Biosensor Fabrication

Ali Akbari Sehat[1], *Abbas Ali Khodadadi*[2,*], *Farzaneh Shemirani*[1*], *Yadollah Mortazavi*[2]

[1] School of chemistry, College of Science, University of Tehran, Tehran, Iran
[2] Catalysis and Nanostructured Materials Research Laboratory, School of Chemical Engineering, University of Tehran, Tehran, Iran.
[*]E-mail: khodadad@ut.ac.ir; shemiran@khayam.ut.ac.ir

Received: 24 August 2014 / *Accepted:* 28 October 2014 / *Published:* 17 November 2014

A fast and simple immobilization of glucose oxidase (GOx) used for fabrication of highly sensitive, quick response (< 2 s) and low cost glucose biosensor. GOx enzyme was immobilized covalently on graphene oxide (GO) modified pencil graphite electrode (PGE) and simultaneously GO was reduced by chronoamperometric and cyclic voltammetric methods. The fabricated biosensor by chronoamperometry showed sharper redox peaks current for GOx in comparison with cyclic voltammetry. Attenuated transmission reflectance (ATR) spectroscopy was used for characterization of covalent immobilization of GOx. The immobilization time of GOx on GO was shortened to 30 s, the minimum immobilization time in other works was 20 minutes, after drying of GO-GOx paste on the PGE. The electrochemical properties of the fabricated biosensor were studied by cyclic voltammetry (CV) and chronoamperometry. The cyclic voltammetric behavior of the fabricated electrode shows a pair of well-defined peaks with a formal potential of -0.521 V and peak to peak separation of 35 mV, indicating direct electron transfer between GOx and electrode. The fabricated biosensor shows a fast electron transfer of k_s=5.84 s^{-1}, a high affinity for glucose with Michaelis-Menten constant K_m = 0.215 mM, a high sensitivity of 278.4 µA mM^{-1} cm^{-2}, a low detection limit of 0.61 µM, and a linear range of 40 to 600 µM. The fast and simple immobilization and GO reduction method can be used in fabrication of other electrochemical biosensors and biofuel cells with low costs.

Keywords: Glucose oxidase, Fast immobilization, High sensitivity, Graphene oxide, Electrochemical biosensor,

1. INTRODUCTION

Diabetes is a worldwide critical health problem that is besides other fatal diseases such as cardiovascular disease and different cancers, threatens the health of communities. Because of high

selectivity, glucose oxidase (GOx) has an important role in real-time detecting of glucose. Electrochemical biosensors are used as glucose detectors in different kinds of samples.

Design of third generation of biosensors is relevant to enzyme immobilization on the surface of the electrode and direct electron transfer from enzyme active sites to the electrode. The poor electrical communication of the active site of the enzyme and the electrode surface accompanied by enzyme leaching are two important problems in enzyme immobilization [1-5]. Flavin adenine dinucleotide (FAD), as a cofactor, is the active site of GOx enzyme [6, 7]. Since FAD is embedded within a protective protein shell, the path length of the electrode to the FAD is too far for a direct electron transfer [8, 9]. Heller has proposed that the maximum distance the electron transfers is about 20 Å and, but the gap of FAD to the electrode surface is more than 25 Å [10]. Therefore, for having an efficient connection between the active site of GOx and the electrode surface, the mediator must be used.

Several methods have been employed for immobilization of GOx on the electrode surface using some mediators such as gold nanoparticles [11], conducting polymer with metal oxide composites [12], CdS and ZnS nanoparticles [13], ionic liquids [14], and carbon nanotubes [15]. All these findings reveal that immobilization matrix with good electrical conductivity, stability and compatible functional groups are necessary for biosensor design. Recently, a new material as graphene has been introduced into the modification of biosensors because of more considerable advantages in immobilization of enzymes on the substrates in contrast with other materials [16-18].

Graphene is the name given to a flat monolayer of carbon atoms tightly packed into a two-dimensional (2D) honeycomb lattice and is a basic building block for graphitic carbon materials of all other dimensionalities [19]. Specific properties of this material have been eventuated to various applications in different fields. Mechanical stability, high intrinsic mobility (200,000 $cm^2\ v^{-1}\ s^{-1}$), high theoretical specific surface area (2630 $m^2\ g^{-1}$), good biocompatibility and chemical stability are some important properties of graphene [20, 21].

In recent years, graphene embodied excellent properties in biosensors and direct electron transfer of enzymes to the electrodes has been magnified owing to large surface area and high intrinsic conductivity. However, graphene sheets could be re-stocked by van der Waals forces of attraction and form graphite [22]. In addition, dispersion of graphene in aqueous media is difficult owing to the hydrophobic nature. So, use of graphene in biosensors design needs versatile strategies to overcome the problems [23-25]. Different strategies for successful immobilization of GOx on graphene [12], graphene nanosheets and carbon nanospheres [26] have been employed. For instance, concanavalin A [27, 28] copper phthalocyanine [29] chitosan–ferrocene [30] and TiO_2 [31] has been used in graphene composites for GOx immobilization. Almost, the immobilization methods involve many steps and need two or more modifiers or additives, such as concanavalin A [27], chitosan-ferrocene [30] and polyethylenimine-functionalized ionic liquid [32]. Use of additives and complex modifiers raise the immobilization steps and therefore complicate the immobilization of the enzyme. In addition, maybe the biosensor lifetime decrease because of side reactions happening during the prolonged immobilization time. Graphene oxide with abundant oxygen functional groups has the potential to decrease the immobilization steps and time by a facile and feasible method without any additives or complex modifiers.

Irreversible and reversible immobilization of enzyme is done by covalent bonding and some non-covalent interactions respectively. Non-covalent interactions, usually through physical adsorption or weak connections occur, but the best immobilization of GOx arises from covalent bonds formation of GOx with modifier because of high stability and non-releasing of the enzyme [5, 33]. For this purpose, modifiers should have some functional groups to bind covalently with GOx free functional groups. GO has many oxygen functional groups to bind with free amino groups of GOx. The influential carboxylic functional groups can bind covalently to free amino groups of GOx [34]. A GO sheet has many carboxylic functional groups at the edge and other oxygen functional groups in the plane. Existence of oxygen functional groups diminishes the electrical conductivity of GO sheet. So, for having good electrical conductivity, oxygen functional groups on the surface of GO should remove. Using electrochemical methods, the surface oxygen functional groups remove, whereas small amount of carboxylic functional groups remain [35]. Short time potential applying in chronoamperometry method (e.g. -1.5 V in < 30 s) causes more carboxylic functional groups remain [35]. Using this method covalent bond forms between free amino group of GOx and the remained carboxylic functional group of GO in a step and therefore, the immobilization time is shortened appreciably.

Selection of working electrode for biosensor fabrication needs some important points that everyone causes some advantages during the work. Low cost, readily available, easily pretreatment, low background current and good conductivity are some important points in the selection of electrode material [36]. Glassy carbon, gold, platinum and some other materials were used as a working electrode in modified biosensors fabrication. But the high price and difficult pretreatment and low availability are as drawbacks of these materials in electrode fabrication.

Pencil graphite is an alternative, low cost and disposable material for the mentioned commercial electrodes. Low background current and good electrical conductivity are some additional features of this material. Different kinds of pencil graphite have been used as an electrode in electrochemical investigations and determinations of some elements and biological materials [37]. The surface properties of this material change with differing degree of hardness. Increasing in hardness degree (4B to 4H types of pencil graphite) causes more disorders on the surface. The kinetics of electron transfer becomes faster when the edge planes increase with diminishing disorders on the surface [38]. For these reasons, the pencil graphite electrode (2B type) was selected for the biosensor fabrication in this work.

In the present study, chronoamperometric and voltammetric methods were applied to GO GOx immobilization with simultaneous reduction of GO. So, in such ways the modified electrodes were prepared. In comparison, of immobilization time and current values of redox peaks of GOx by these two methods, the results indicated that the immobilization time decreased significantly using chronoamperometry method and the redox peak currents increased, effectively. Reducing many steps of GOx immobilization to single step and omitting of the additives came about by using this method. The modified RGO-GOx electrode was used to sensitive detection of glucose.

2. EXPERIMENTAL

2.1 Materials

An extra pure graphite powder was obtained from Merck. Glucose oxidase (GOx) Aspergillus Niger (130 U/mg) was purchased from Fluka. β-D (+) -Glucose was supplied by the Sigma Chemical Company. All other chemicals were supplied from Merck. 0.1 M phosphate buffer solution (PBS) was prepared from 0.1 M Na_2HPO_4 and NaH_2PO_4 and the pH was adjusted to 7. Inert atmosphere was set by passing N_2 through the solution during the electrochemical experiments.

2.2 Apparatus and measurements

The cyclic voltammetry and chronoamperometry experiments were carried out with a PalmSens3 Potentiostat/Galvanostat (Ivium, The Netherland). A conventional three electrode system, including the modified PGE as the working electrode, a thin PT wire as a counter electrode, and an Ag/AgCl (in saturated KCl) as reference electrode was used. Transmission electron microscopy (TEM) was performed by using a Philips (Model CM120, 120kV, The Netherland) transmission electron microscope. Attenuated reflectance spectroscopy (ATR) measurements were performed by using a Bruker tensor 27 FT-IR spectrometer (Germany). Raman spectra were obtained from Almega Thermo Nicolet Dispersive Raman Spectrometer applying 532 nm laser's light (The USA).

2.3 Preparation of graphene oxide

Graphite oxide was synthesized from the graphite fine powder by the modified Hummers method [39]. The pristine graphite oxidized by potassium permanganate in concentrated acidic solution. The remaining potassium permanganate neutralized by hydrogen peroxide solution and as-prepared graphite oxide washed with deionized water several times. After drying, the as-prepared graphite oxide was dispersed in deionized water (0.5 mg/mL) and exfoliated by probe ultrasonic for 15 minutes to produce GO solution.

2.4 Fabrication of PGE/RGO-GOx modified electrode

Before electrode modification, the pencil graphite electrode (PGE, Micro, 2B, 0.9 mm diameter, and surface area of 6.36×10^{-3} cm^2, made in Korea) was polished by a glossy paper sheet and then treated by applying +1.8 V oxidation potential in 1 M NaOH solution for 10 s. The as-prepared electrode washed with deionized water to remove residual NaOH from the surface of the electrode. 2 µL of GO solution (0.5 mg/mL) was drop cast on the prepared PGE and kept at room temperature to dry. 2 µL of GOx solution (5 mg/mL in 0.1 M PBS, pH 7) was drop cast onto dried GO and was kept at 15±3^oC for 5 minutes. The immobilization of GOx with simultaneous reduction of GO was done by two electrochemical methods for two fabricated electrodes. In the first method, continuous cyclic voltammetry (6 cycles from 0 to -1.5 V at scan rate of 50 mV s^{-1}) was employed and in the second

method the constant potential of -1.5 V was applied for 30 s. Finally, the as-prepared modified electrodes were rinsed with deionized water to remove any weakly attached GOx or GO. The modified electrodes are identified as PGE/RGO-GOx.

3. RESULTS AND DISCUSSIONS

3.1. Characterization of graphene oxide

Figure 1A represents the TEM micrograph of the graphene oxide (GO). The wrinkling in GO sheets and the contrast, in comparison with the background, indicates that the synthesized GO comprises few layers (1-3 layers) [40]. Figure 1B shows the Raman spectrum of GO. The appearance of 2D peak at 2740 cm^{-1} and the overtone of D band deduce that GO contains a few graphene layers [41]. The peak at 2938 cm^{-1} presents C-H bonds in the GO structure because of the defect bands in GO layers and acidic media used during synthesis of GO [40]. The peak at 3165 cm^{-1} is attributed to hydroxyl and carboxylic functional groups owing to the formation of OH bonds in GO layers. The D-band peak at 1360 cm^{-1} indicates the formation of defects in crystalline structure of graphite. The defects in crystalline graphite increase with raising the ratio of I_D/ I_G. This is owing to separating of GO layers and stretching the bonds in honeycomb lattice in the plane of GO [40].

According to NMR and neutron scattering studies, the water remains amongst GO planes in a wide range of temperatures (123-473 K) [42]. This indicates the hydrogen bond formation of epoxy functional groups of the GO basal planes and water molecules. This is the reason for stacking of the GO sheets and formation of a few layers GO.

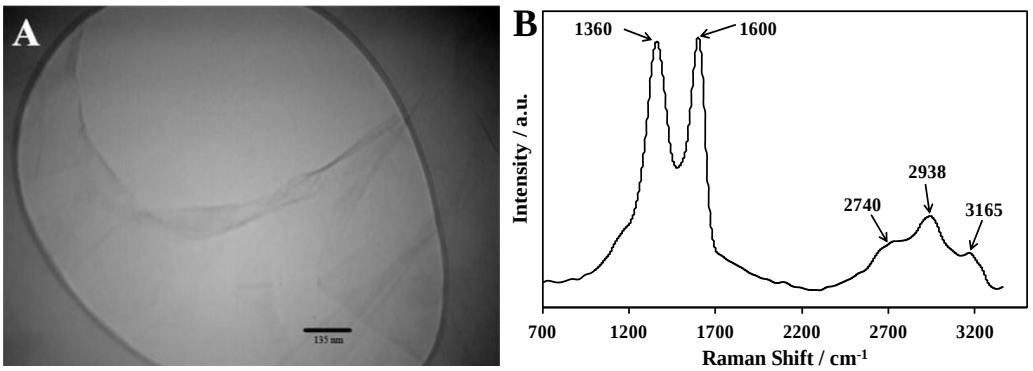

Figure 1. (A) TEM image of graphene oxide. (B) Raman spectrum of graphene oxide.

3.2. Simultaneous electrochemical reduction of GO and immobilization of GOx

3.2.1. Cyclic voltammetric reduction of GO and its functional groups

Figure 2A shows the typical electrochemical reduction of GO by the cyclic voltammetry method. A broad GO reduction peak appeared at -1.061 V is related to the reduction of oxygen

functional groups on GO. Based on location of functional groups in GO plane, carboxylic functional groups, often are at the edge and the other groups such as epoxy and hydroxyl are on the basal plane of GO. Most of non-carboxylic groups are removed in potentials smaller than -1.0 V, whereas the carboxylic groups need potentials more negative than -1.0 V. By raising the negative potential value from -1.0 to -1.5 V, large amounts of carboxylic groups are removed from the GO planes [35]. Carboxylic functional groups are able to bind covalently to free amino groups of GOx [34], but the amounts of remaining carboxylic groups are not considerable for the formation of numerous covalent bonds with free amino groups of GOx. For this reason, the simultaneous reduction of GO and GOx immobilization was employed in the formation of large numbers of covalent bonds.

3.2.2. Cyclic voltammetric and chronoamperometric immobilization of GOx on GO

Immobilization of GOx on GO is created by chemical and electrochemical methods. In chemical methods some additional reagents or specific conditions are necessary [30, 32]. On the other hand, in electrochemical methods GOx immobilization could occur without any additional reagents or specific conditions.

Cyclic voltammetry is the first electrochemical method for immobilization of GOx on GO sheets. Figure 2B shows the simultaneous reduction of GO and GOx immobilization on GO by the continuous cyclic voltammetry. In the first cycle, a broad cathodic peak appeared with an onset potential of about -0.8 V is attributed to the reduction of oxygen functional groups of GO [35]. Reduction peak of GO in Figure 2B has few similarities in comparison with Figure 2A. The difference probably depends on participation of H^+ reduction in the presence of GOx in GO/GOx composite. In the consecutive cyclic voltammograms the cathodic peak decreases and redox peaks of GOx appear clearly (Inset of Figure 2B). The as-prepared modified electrode is identified as PGE/ RGO-GOx. Before usage, the modified electrode is scanned from -0.6 V to +0.6 V by cyclic voltammetry for two cycles owing to remove of negatively charge residuals during the electrode modification. The modification procedure was repeated for several electrodes and the obtained continuous cyclic voltammograms of these electrodes were similar to the first as explained.

Chronoamperometry is the second electrochemical method for immobilization of GOx on the GO sheets. Three PGE/GO-GOx electrodes prepared and used to find optimum time of simultaneous reduction of GO and immobilization of GOx at -1.5 V applied potential. Figure 2C shows a simultaneous reduction of GO and immobilization of GOx on GO sheets by chronoamperometry for three electrodes. For all three electrodes, a sharp change is observed in reduction current during the first 5 s. The next significant change appears during the second 5 s and after 20 s the current becomes steady. In the electrode number 3, the reduction current has two peaks following by steady current these may be related to more functional groups on GO. These changes are attributed to reduction of GO and immobilization of GOx on the surface of the electrode and where the current becomes steady indicates the optimum time (30 s) for preparation of the modified electrode. The mentioned procedure was repeated for several electrodes and the optimum times were similar.

3.2.3. ATR spectroscopic study of RGO-GOx composite

During the oxidation of graphite to GO, different types of oxygen functional groups form on GO surface. ATR spectra in the infrared region can reveal the functionalities by measuring the different types of bond vibrations. Figure 2D shows the ATR spectra of GO, RGO, GOx and RGO-GOx composite. The GO spectrum, the curve (a), exhibits a broad peak at 3400 cm^{-1}, demonstrating the O-H stretching vibrations of the carboxylic acid functional group. Peak at 1736 cm^{-1} is due to C=O bond formation during oxidation reaction. The C=C skeletal vibrations appear at 1630 cm^{-1} because of unoxidized graphitic domains.

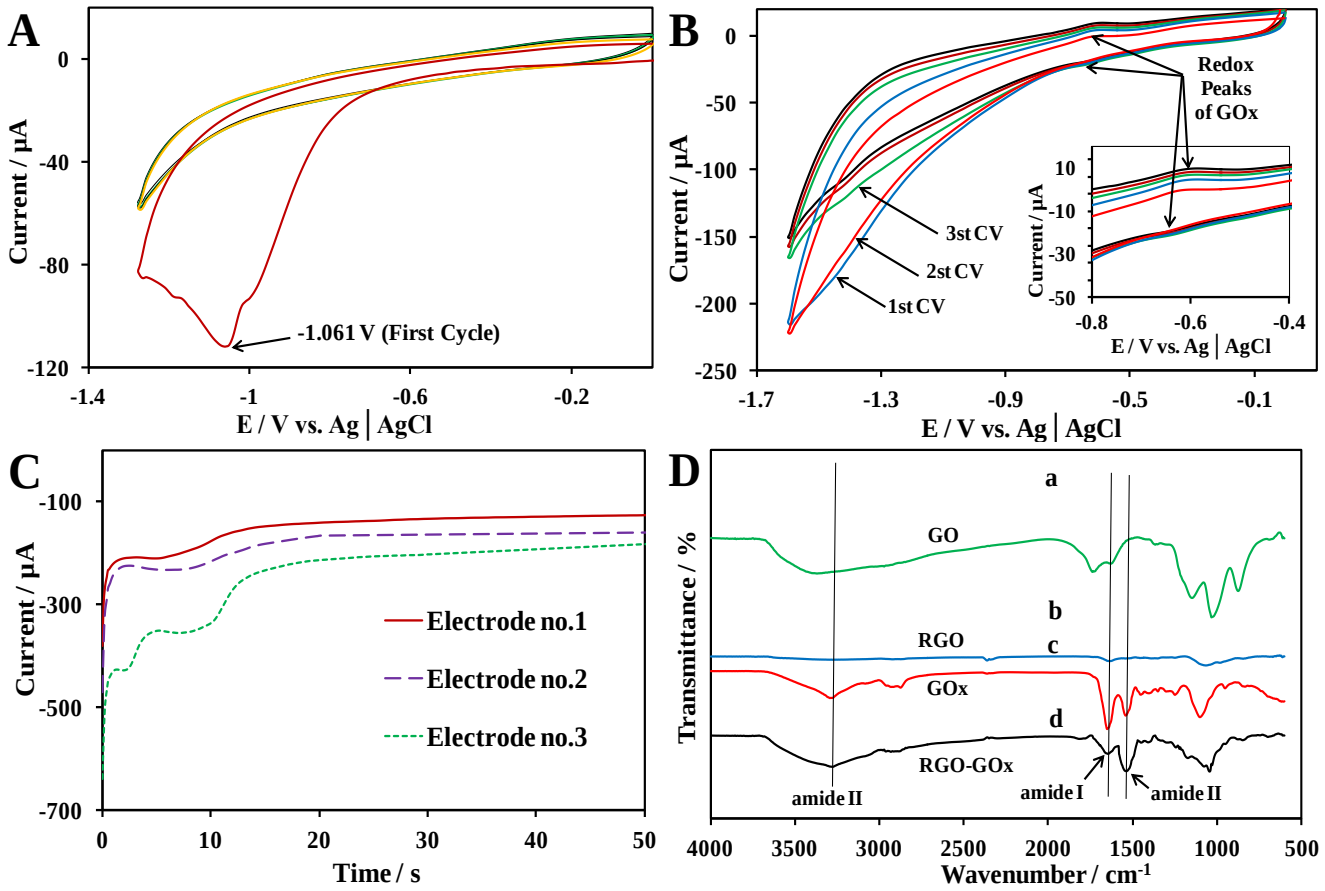

Figure 2. (A) Cyclic voltammetry reduction of GO to RGO. (B) Simultaneous cyclic voltammetry reduction of GO and immobilization of GOx to RGO-GOx (Inset plot: The magnified redox peaks of GOx). (C) Simultaneous chronoamperometry reduction of GO and immobilization of GOx by applied potential of -1.5 V vs. Ag/AgCl reference. (D) ATR spectra of (a) GO, (b) RGO, (c) GOx and (d) RGO-GOx.

The stretching peak of C-OH bond was overlapped by vibrations of alkoxy C-O functional group at 1147 cm^{-1}. The peak at 1031 cm^{-1} corresponds to C-O-C or C-O vibrations and the epoxy functional group vibrations appear at 874 cm^{-1} [43]. Curve (b) shows the spectrum of RGO from GO in pH 7 by applying potential at -1.5 V for 30 s by chronoamperometry. As the figure shows the peak at

3400 cm^{-1} (C-OH stretching) disappears, indicating the reduction of hydroxyl groups. Also, the other functional groups peaks disappear or become insignificant attributing to remove almost all functionalities. As the GOx spectrum is shown in curve (c) the peaks at 3292 cm^{-1} is ascribed to N-H stretching vibrations in amide (II). The peaks at 2929 cm^{-1} and 2873 cm^{-1} represent C-H stretching bands. The most important peaks of GOx are the N-H bending peak appeared at 1540 cm^{-1} for amide (II) and the C=O stretching peak at 1649 cm^{-1} for amide (I). The peak at 1100 cm^{-1} is related to R-C=O (acyl group) or C-O (alkoxy group) stretching vibrations. At 1030 cm^{-1} the peak of C-N stretching is shown that is covered by acyl group peak. When the potential of -1.5 V is applied to GO-GOx composite, a significant peak is revealed at 1030 cm^{-1} indicating the C-N stretching band. In comparison with GOx spectrum, the amide (I) peak decreases at 1627 cm^{-1} (with 22 cm^{-1}) considerably, while the amide (II) peak increases at 1535 cm^{-1} (with 5 cm^{-1} shift) significantly for RGO-GOx spectrum. These results indicate that covalent bond between free amino group of GOx and the carboxylic group of RGO is formed.

3.2.4. Comparison of direct electrochemistry of PGE/RGO-GOx modified electrodes fabricated by cyclic voltammetry and chronoamperometry

After application of the two modification methods, as being raised in the section 3.2.2, the direct electrochemistry of PGE/GOx-RGO electrode is investigated by cyclic voltammetry in N_2 saturated PBS (pH=7) in the potential range -0.2 to -0.7 V at scan rate 50 mV s^{-1}. The results are presented in Figure 3A, Curve (a), shows the cyclic voltammogram of GOx/RGO after continuous cyclic voltammetric modification method. Curves (b), (c) and (d) show the cyclic voltammograms of the three PGE/GOx-RGO electrodes modified by chronoamperometry during the times 10, 20 and 30 s respectively. The cyclic voltammograms for the three modified electrodes show the redox peak of GOx is more specified and repeatable after 20 s. Owing to the higher cathodic (I_{pc}) and anodic (I_{pa}) peak currents, the chronoamperometric method has better results in comparison with continuous cyclic voltammetry modification and therefore this method was performed for all subsequent experiments.

For obtaining the maximum possible current in direct electron transfer, mass ratio of GO to GOx has been optimized. The best ratio was obtained 1 μg of GO and 10 μg of GOx and was used for all experiments in this work.

A comparison of bare PGE, PGE/RGO and PGE/RGO-GOx electrodes CVs are presented in Figure 3B. The bare PGE shows no peak in the absence of GOx (curve a) and PGE/RGO shows a more specific area without GOx immobilization (curve b). The ratio of the anodic peak current (I_{pa}) to the cathodic peak current (I_{pc}) is approximately 1. The modified PGE/RGO-GOx electrode shows a well-defined redox couple with a peak to peak separation (ΔE_p) of 37 mV at scan rate of 50 mV s^{-1}. The ΔE_p value indicates a reversible and fast electron transfer process. In comparison with other works, the redox peak currents are higher because of the greater surface coverage concentration (Γ) of 1.84×10^{-9} mol GOx cm^{-2} on the PGE/RGO-GOx [28-31]. The calculated value of Γ obtained from the equation, $\Gamma = Q/nFA$. Where Q is the charge of oxidation peak (2.2565×10^{-6} C), n is the transferred electrons number (n=2), F is the Faraday constant (96485.34 C mol^{-1}) and A is the PGE surface area (6.36×10^{-3} cm^{-2}) [44, 45]. The calculated Γ value is bigger than the theoretical value of 2.86×10^{-12} mol cm^{-2} for

monolayer GOx on the bare electrode surface [44]. This indicates that the multilayer coverage of GOx contributes to direct electron transfer at the electrode surface. The multilayer immobilization of GOx at the surface of the electrode could be attributed to greater participation of edge of GO planes in GOx immobilization.

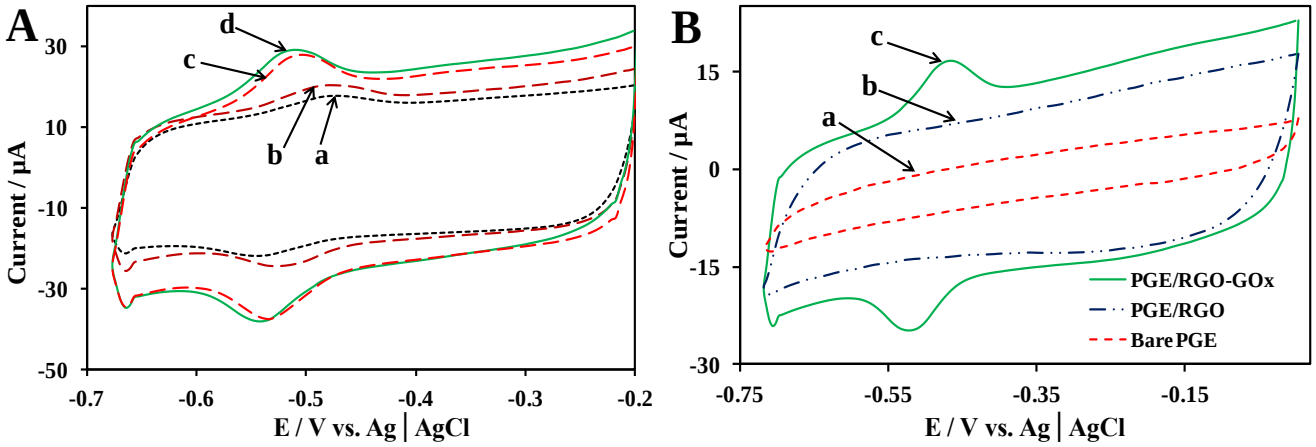

Figure 3. (A) CVs of PGE/RGO-GOx: (a) after (B) process, (b), (c) and (d) after (C) process for 10, 20 and 30 s, respectively. All experiments in N_2 - saturated PBS 0.1 M pH 7 and CVs, scan rate 50 mVs^{-1}. (B) Cyclic voltammogram in N_2 - saturated PBS 0.1 M pH 7 of a) Bare PGE electrode b) PGE/RGO electrode and c) PGE/RGO-GOx electrode. Scan rate 50 mVs^{-1}.

3.3 Effect of scan rate

The influence of scan rates on redox peaks of PGE/RGO-GOx is shown in Figure 4. From scan rates of 20 to 300 mV s^{-1} the cathodic peak current (I_{pc}) and anodic peak current (I_{pa}) increase linearly with the scan rate increase (Inset of Figure 4). This is attributed to the reversible surface control of GOx electrochemical reaction. Both cathodic and anodic peak potentials of GOx shift slightly, whereas the formal redox potentials ($E^{0'}$) of GOx almost remain unchanged. The apparent heterogeneous electron transfer rate constant (k_s) of GOx at PGE/RGO-GOx is calculated from Laviron equation 1 (for $n\Delta E_p < 200$) [44]:

$$k_s = \frac{(1-\alpha)nF\nu}{RT} \qquad (1)$$

Where α is the charge transfer coefficient is assumed ≈ 0.5 and n is the transferred electrons number is assumed 2. ΔE_p is the peak separation of the FAD/$FADH_2$ redox couple obtained 97 mV at scan rate of 150 mV s^{-1}, T is the room temperature (298.15 K) and R is the universal gas constant (8.314 J mol^{-1} K^{-1}). The calculated rate constant (k_s) for electron transfer of GOx at PGE/RGO-GOx is 5.84 s^{-1}, indicating fast electron transfer process. Hence, the obtained result could be related to more edge sites of RGO planes participating in electron transfer kinetics process [45, 46].

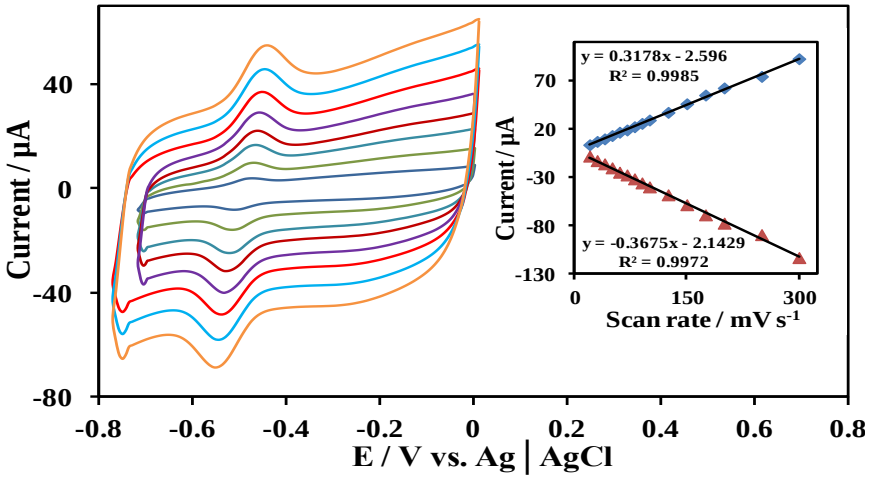

Figure 4. Cyclic voltammogram of RGO-GOx in N_2 - saturated PBS 0.1 M pH 7 at different scan rates from 20 to 300 mV s^{-1} in N_2 - saturated PBS 0.1 M pH 7. Inset plot is the linear corrolation between different scan rates from 20 to 300 mV s^{-1} and peak currents in N_2 - saturated PBS 0.1 M pH 7.

3.4 Effect of pH

The influence of pH on the electrochemical behavior of FAD/$FADH_2$ at PGE/RGO-GOx is shown in Figure 5. The CVs of the modified electrode are recorded at different pH values of 4, 5, 6, 7, 8 and 9. The CVs show stable well-defined redox peaks for GOx, indicating the direct electron transfer and high activity of GOx at different pH values. The formal redox potential of GOx shifts to more negative values, as the pH increases. This implies that the easier redox process of GOx at low pH accompanies protonated process. Inset of Figure 5 shows the linear dependence of the formal redox potential of GOx to pH with a slope of -55.8 mV/ pH that is close to the theoretical value of Nerstian equation for two electrons and two protons transfer in electrochemical processes.

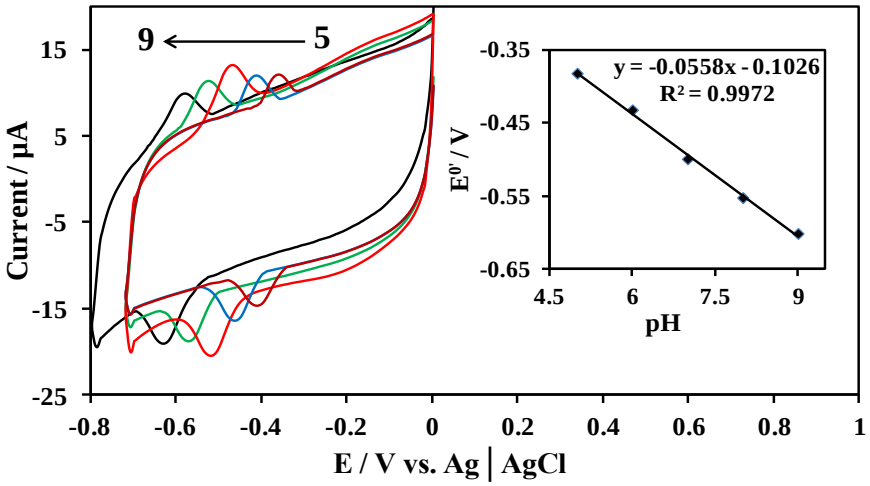

Figure 5. Cyclic voltammograms of RGO-GOx in N_2 - saturated PBS at different pH values from 5 to 9, scan rate 50 mV s^{-1}. Inset plot is correlation between pH value and formal potential of RGO-GOx in N_2 - saturated PBS.

3.5 Electrocatalytic activity of PGE/RGO-GOx toward O_2 and glucose

The activity of the modified PGE/RGO-GOx electrode toward O_2 is related to the consumption of O_2 in PBS. The GOx in the modified film is in the form of FAD and reduces to $FADH_2$ according equation (2) and is oxidized to FAD form, according equation (3). Increasing of O_2 concentration from N_2-saturated to O_2-saturated, show significant increase in the reduction peak current and decrease in the oxidation peak current (see Figure 6A, a to c) respectively. In equation (3) FAD is regenerated for successive reactions. The reaction equations are as follows:

$$GOx\ (FAD) + 2H^+ + 2e^- \rightleftharpoons GOx\ (FADH_2) \quad (2)$$

$$GOx\ (FADH_2) + O_2 \longrightarrow GOx\ (FAD) + H_2O_2 \quad (3)$$

As glucose is added to PBS, the reduction peak current of GOx decreases because of consumption of glucose in oxidation reaction to the gluconolactone, according to the following equation:

$$GOx\ (FAD) + glucose \longrightarrow GOx\ (FADH_2) + gluconolactone \quad (4)$$

3.6 Amperometric determination of glucose at PGE/RGO- GOx modified electrode

Determination of glucose on the modified electrode surface was done by amperometric method. To obtain high sensitivity in the amperometric determination of glucose samples, the applied potential was optimized with different potentials from -0.3 V to -0.6 V in air- saturated PBS 0.1 M (pH=7) as shown in Figure 6B. The reduction current of the modified electrode increases quickly after each addition of glucose to the stirred PBS. Moreover, the reduction current increases with increasing applied potentials and maximizes at -0.6 V. This value is the optimum potential for determination of glucose. The response time of the modified electrode to the added glucose is fast (less than 2 s) and the current response becomes stable in less than 25 s. By applying -0.6 V optimum applied potential, the calibration curve of the modified PGE/ RGO-GOx electrode to different glucose concentrations was obtained in air- saturated PBS 0.1 M (pH=7) as shown in Figure 7A . Before glucose addition, at -0.6 V applied potential that is less than onset potential of GOx ($FADH_2$) oxidation (-0.55 V), GOx (FAD) reduces to GOx ($FADH_2$). $FADH_2$ is oxidized to FAD form by dissolved O_2 in PBS, according to equation (3) and the current becomes steady with consideration to the equation (2). By addition of glucose to PBS, more amount of produced FAD is reduced to $FADH_2$ and therefore the reduction peak current increases. The obtained calibration curve shows that the current increase is proportional to the concentration of glucose in solution. The linear range of the calibration curve is from 40 μM to 600 μM glucose with the regression equation of $I(\mu A) = -1.91 - 0.0018 C_{glucose}(\mu M)$ and correlation coefficient of 0.9975 (Inset of Figure 7A). Based on the calculated slope of the calibration curve (1.8 μA mM^{-1}) the fabricated biosensor exhibits a high sensitivity of 278.4 μA mM^{-1} cm^{-2} for ≈ 6.36×10^{-3} cm^2 surface area of PGE. The high sensitivity of the modified electrode to glucose indicates well biocatalytic activity and conductivity of the RGO. The obtained detection limit for glucose determination is 0.61 μM with signal to noise ratio of 3.0 using the equation $3S_b/S$, where S_b is the standard deviation of the blank signal (0.057 μA) and S is the sensitivity [47]. The detection limits' low value is attributed to the low noise background current and high sensitivity of the biosensor. The

Michaelis-Menten constant (K_m^{app}), which is indicative of both the ratio of microscopic kinetic constant and the enzymatic affinity, was calculated 0.215 mM according to the Lineweaver-Burk equation [48]. The additional comparison of the fabricated biosensor in this work with other glucose biosensors based on GOx is shown in Table 1. The results show that the fabricated biosensor exhibited higher sensitivity and electron transfer kinetic process while the Michaelis-Menten constant and detection limit reduced in this work in comparison with other similar works [45, 46, 49-54]. The high performance of the biosensor could be attributed to the covalent bond formation of free amino functional groups of GOx with carboxylic ones on the GO edges. Furthermore, the higher concentrations of carboxylic functional groups on the edges of highly oxidized graphene sheets can enhance the total amount of GOx loading on RGO sheets.

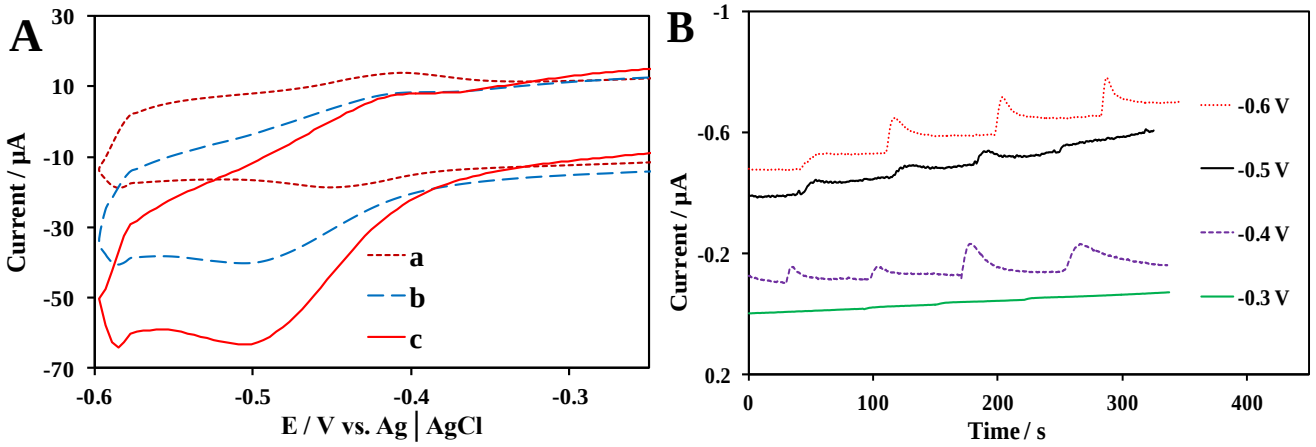

Figure 6. (A) Cyclic voltammogram of PGE/ RGO-GOx in PBS 0.1 M pH 7 for a) in N_2-saturated b) air-saturated and c) O_2-saturated, scan rate 50 mV s^{-1}. (B) Amperometric response of the modified electrode to glucose at different potential values from -0.3 to -0.6 V vs. Ag/AgCl reference in air - saturated PBS 0.1 M, pH 7.

Table.1. Comparison of the results of the fabricated biosensor with some similar works.

Modified electrode	Sensitivity (µA mM^{-1} cm^{-2})	Detection Limit (µM)	Heterogeneous electron transfer k (s^{-1})	Linear range	Immobilization time	Reference
GOx /Graphene/GCE	110	10	2.68	0.1-10 mM	1 hour	[45]
GOx/Chitosan-Graphene/GCE	37.93	20	2.83	0.08-12 mM	-	[46]
GOx/Graphene-Ppy /GCE	-	3	-	2-40 µM	-	[49]
GOx/AuNP -P2VP /ITO	1.51	5600	2.93	2-16 mM	12 hours	[50]
GOx/Carbon-PANI/GCE	-	0.05	-	0.5-10 µM	-	[51]
GOx/SWCNTs - Os(III)LCl2) /GC	826.3	0.056	-	1-1000 µM	26 minutes	[52]

GOx/Chitosan-Au-CdS/ITO	5.9	38	-	50-500 µM	12 hours	[53]
GOx/Fe_3O_4/RGO/GCE	-	50	4.96	0.5-12 mM	2 hours	[54]
RGO-GOx/PGE	278.4	0.61	5.84	40-600 µM	5 minutes drying + 30 s immobilization	This work

3.7 Selectivity, stability, reproducibility of the biosensor

For investigation of the selectivity of the fabricated biosensor for glucose, interfering species was studied by using of ascorbic acid (AA) and uric acid (UA). Addition of 0.5 mM of AA and UA in 0.1 M PBS in amperometric detection did not cause any significant signal, while 0.1 mM glucose addition in 0.1 M PBS resulted in a considerable signal (Figure 7B). This indicates high selectivity for glucose, but no interference of AA and UA of the biosensor. Stability of the biosensor was investigated by recording of 30 CVs of PGE/RGO-GOx in 0.1 M PBS without any significant decrease of peak currents. Furthermore, for stability test of the biosensor, the CV of modified electrode was recorded after three weeks and the results represented about 6% decrease in cathodic peak current. Reproducibility of the biosensor was investigated by five different as-prepared electrodes with recording the CVs. The relative standard deviation (RSD) of cathodic peak current of electrodes was obtained 4.3% (for n=3), indicating that the immobilization GOx in the biosensor is stable and repeatable. The good repeatability of the prepared modified electrodes could be attributed to the covalent immobilization of GOx on GO sheet by applying of potential without any more additional chemicals.

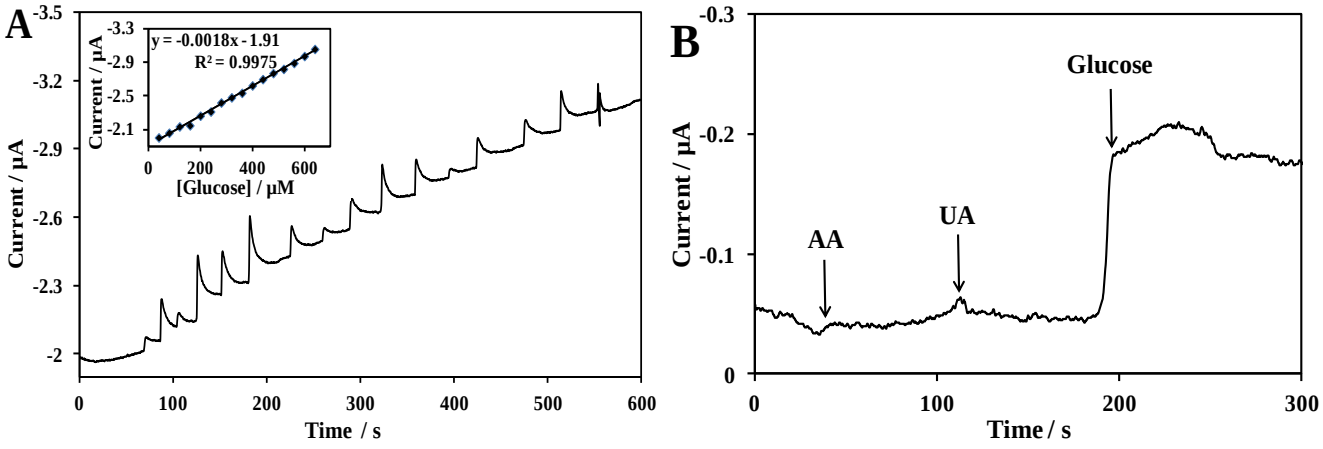

Figure 7. (A) Amperometric response of PGE/RGO-GOx to the continual additions of 1 mM glucose into air- saturated PBS 0.1 M pH 7, -0.6 V applied potential vs. Ag/AgCl reference. Inset is the linear calibration curve of the electrode. (B) Amperometric response of the PGE/RGO-GOx electrode to 0.5 mM ascorbic acid (AA), 0.5 mM uric acid (UA) and 0.1 mM glucose concentrations in air-saturated PBS 0.1 M pH 7, -0.6 V applied potential vs. Ag/AgCl reference.

4. CONCLUSION

We fabricated a highly sensitive, quick response and low cost glucose biosensor with low detection limit. The modified electrode was prepared by electrochemical reduction of GO simultaneously with fast immobilization of glucose oxidase (GOx) without using any additives on pencil graphite electrode (PGE). By applying a constant potential at -1.5 V for 30 s in chronoamperometric method, the GOx redox peak currents increase dramatically. This indicates a simultaneous reduction of GO and immobilization of GOx amongst graphene layers without re-stacking to graphite. The fabricated biosensor shows a high sensitivity of 278.4 μA mM^{-1} cm^{-2} with a low detection limit of 0.61 μM. The sensitivity of the biosensor is significantly higher in comparison with the other similar works. This is attributed to covalent bond formation of free amino functional groups of GOx and carboxylic ones' on the edges of GO with a high loading of GOx. In addition, the biosensor is selective to glucose in the presence of ascorbic acid and uric acid. The new method employed for simultaneous reduction of GO and immobilization of GOx, is a robust procedure for fabrication of carbon based biosensors.

ACKNOWLEDGEMENTS
Financial support from university of Tehran is gratefully acknowledged.

References

1. J. L. House, E. M. Anderson, W. K. Ward, *J. Diabetes Sci. Technol*., 1(2007) 18.
2. X. Yang, L. Huaa, H. Gonga, S. N. Tan, *Anal. Chim. Acta*., 478 (2003) 67.
3. W. Tischer and F. Wedekind, *Topics in current chemistry*, Vol. 200, Springer Verlag, Berlin Heidelberg, (1999).
4. S. Datta, L. R. Christena ,Y. Rani and S. Rajaram, *3 Biotech*., 3 (2013) 1.
5. J. M. Guisan, *Methods in Biotechnology: Immobilization of Enzymes and Cells*, 2 st ed., (Eds.: J. M. Guisan), Humana Press Inc, Totowa, NJ, (2006).
6. S. B. Bankar, M. V. Bule, R. S. Singhal, L. Ananthanarayan, *Biotechnol. Adv*., 27 (2009) 489.
7. Q. H. Gibson, B. E. P. Swoboda, V. Massey, *J. Biol. Chem*., 239 (1964) 3927.
8. R. A. Marcus, N. Sutin, *Biochim. Biophys. Acta*., 811 (1985) 265.
9. A. Heller, *Acc. Chem. Res*., 23 (1990) 128.
10. A. C. Harper, *Modified Electrodes for Amperometric Determination of Glucose and Glutamate Using Mediated Electron Transport*, Univ. Virginia Polytechnic Institute and State University, (2005).
11. C. Qiua, X. Wang, X. Liub, S. Houc, H. Ma, *Electrochim. Acta*., 67 (2012) 140.
12. C. X. Guo, C. M. Li, *Phys. Chem. Chem. Phys*., 12 (2010) 12153.
13. J. Du, X.Yu, J. Di, *Biosens. Bioelectron*., 7 (2012) 88.
14. X. Shangguan, H.g Zhang, J. Zheng, *Electrochem. Commun*., 10 (2008) 1140.
15. Y. Liu, M. Wang, F. Zhao, Z. Xu, S. Dong, *Biosens. Bioelectron*., 21 (2005) 984.
16. M. Y. Elahi, A. A. Khodadadi, Y. Mortazavi, *J. Electrochem. Soc*., 161 (2014) B81.
17. M. F. Hossain, J. Y. Park, *Electroanalysis*., 26 (2014) 940.
18. S. Palanisamy, S. Cheemalapati, S. M. Chen, *Mater. Sci. Eng. C*., 34 (2014) 207.
19. A. K. Geim, K. S. Novoselov, *Nat. Mater*., 6 (2007) 183.
20. K.I. Bolotin, K.J. Sikes, Z. Jiang, M. Klima, G. Fudenberg, J. Hone, P. Kim, H.L. Stormer, *Solid State Commun*., 146 (2008) 351.

21. S.V. Morozov, K. S. Novoselov, M. I. Katsnelson, F. Schedin, D. C. Elias, J. A. Jaszczak, A. K. Geim, *Phys. Rev. Lett*., 100 (2008) 1.
22. D. Li, M. B. Muller, S. Gilje, R. B. Kaner, G. G. Wallace, *Nat. Nanotechnol*., 3 (2008) 101.
23. Y. Shao, J. Wang, H. Wu, J. Liu, I. A. Aksay, Y. Lin, *Electroanalysis*., 22 (2010) 1027.
24. S. Mao, K. Yu, J. Chang, D. A. Steeber, L. E. Ocola, J. Chen, *Sci. Rep*., 1696 (2013) 1.
25. T. Kuila, S. Bose, P. Khanra, A. K. Mishra, N. H. Kim, J. H. Lee, *Biosens. Bioelectron*., 26 (2011) 4637.
26. H. Yin, Y. Zhou, X. Meng, K. Shang, S. Ai, *Biosens. Bioelectron*., 30 (2011) 112.
27. L. Zhou, Y. Jiang, J. Gao, X. Zhao, L. Ma, Q. Zhou, *Biochem. Eng. J*., 69 (2012) 28.
28. J. Huang, L. Zhang, R. P. Liang, J. D. Qiu, *Biosens. Bioelectron*., 41 (2013) 430.
29. Y. Q. Zhang, Y. J. Fan, L. Cheng, L. L Fan, Z. Y. Wang, J. P. Zhong, L. N Wu, X. C. Shen, Z. J. Shi, *Electrochim. Acta*., 104 (2013) 178.
30. J. D. Qiu, J. Huang, R. P. Liang, *Sens. Actuators, B*., 160 (2011) 287.
31. H. D. Jang, S. K. Kim, H. Chang , K. M. Roh, J. W. Choi, J. Huang, *Biosens. Bioelectron*., 38 (2012) 184.
32. C. Shan, H. Yang, J. Song, D. Han, A. Ivaska, L. Niu, *Anal. Chem*., 81 (2009) 2378.
33. R. A. Sheldon, *Adv. Synth. Catal*., 349 (2007) 1289.
34. Y. Liu, D. Yu, C. Zeng, Z. Miao, Liming Dai, *Langmuir*., 26 (2010) 6158.
35. H. L. Guo, X. F. Wang, Q. Y. Qian, F. B. Wang, X. H. Xia, *ACS Nano*., 3 (2009) 2653.
36. D. Demetriades, A. Economou, A. Voulgaropoulos, *Anal. Chim. Acta*., 519 (2004) 167.
37. R. Navratil, I. Pilarova, F. Jelen, L. Trnkova, *Int. J. Electrochem. Sci*., 8 (2013) 4397.
38. J. K. Kariuki, *J. Electrochem. Soc*., 159 (2012) H747.
39. D. C. Marcano, D. V. Kosynkin, J. M. Berlin, A. Sinitskii, Z. Sun, A. Slesarev, L. B. Alemany, W. Lu, J. M. Tour, *ACS Nano*., 8 (2010) 4806.
40. K. S. Hazra, J. Rafiee, M. A. Rafiee, A. Mathur, S. S. Roy, J. McLauhglin, N. Koratkar, D. S. Misra, *Nanotechnology*. 22 (2011) 025704.
41. A. C. Ferrari, J. C. Meyer, V. Scardaci, C. Casiraghi, M. Lazzeri, F. Mauri, S. Piscanec, D. Jiang, K. S. Novoselov, S. Roth, A. K. Geim, *Phys. Rev. Lett*., 97 (2006) 187401.
42. D. R. Dreyer, S. Park, C. W. Bielawski, R. S. Ruoff, *Chem. Soc. Rev*., 39 (2010) 228.
43. Y. Jiang, Q. Zhang, F. Li, L. Niu, *Sens. Actuators, B*., 161 (2012) 728.
44. E. Laviron, *J. Electroanal. Chem*., 101 (1979) 19.
45. P. Wu, Q. Shao, Y. Hu, J. Jin, Y. Yin, H. Zhang, C. Cai, *Electrochim. Acta*., 55 (2010) 8606.
46. X. Kanga, J. Wang, H. Wu, I. A. Aksay, J. Liu, Y. Lin, *Biosens. Bioelectron*., 25 (2009) 901.
47. A. Radoi, D. Compagnone, E. Devic, G. Palleschi, *Sens. Actuators, B*., 121 (2007) 501.
48. R. A. Kamin, G. S. Wilson, *Anal. Chem*., 52 (1980) 1198.
49. S. Alwarappan, C. Liu, A. Kumar, C. Z. Li, *J. Phys. Chem. C*., 114 (2010) 12920.
50. B. P. Crulhas, J. R. Sempionatto, M. F. Cabral, S. Minko, V. A. Pedrosa, *Electroanalysis*., 26 (2014) 815.
51. Ö. Çolak, H. Arslan, H. Zengin, G. Zengin, *Int. J. Electrochem. Sci*., 7 (2012) 6988.
52. A. Salimi, B. Kavosi, R. Hallaj, A. Babaei, *Electroanalysis*., 21 (2009) 909.
53. J. Qian, S. Yan, Z. Xiao, *J. Colloid Interface Sci*., 366 (2012) 130.
54. H. Teymourian, A. Salimi, S. Firoozi, *Electroanalysis*., 26 (2014) 129.